Chelation-Based Stabilization of the Transition Structure in a Lithium Diisopropylamide Mediated Dehydrobromination: Avoiding the "Universal Ground State" Assumption

Julius F. Remenar and David B. Collum*

Contribution from the Department of Chemistry, Baker Laboratory, Cornell University, Ithaca, New York 14853-1301

Received January 3, 1997[⊗]

Abstract: Dehydrobrominations of (±)-2-*exo*-bromonorbornane (RBr) by lithium diisopropylamide (LDA) were investigated to determine the roles of aggregation and solvation. Elimination with LDA/*n*-BuOMe occurs by deaggregation of disolvated dimers via a monosolvated monomer transition structure (e.g., [*i*-Pr$_2$NLi·*n*-BuOMe·-RBr]‡). In contrast, elimination by LDA−THF displays THF concentration dependencies that are consistent with parallel reaction pathways involving both mono- and disolvated monomer transition structures. Elimination is markedly faster by LDA−DME than by LDA with monodentate ligands and follows a rate law consistent with a transition structure containing a chelated monomeric LDA fragment. A number of hemilabile amino ethers reveal the capacity of different coordinating functionalities to chelate. A protocol based upon kinetic methods affords the relative ligand binding energies in the LDA dimer reactants. Separating contributions of ground state from transition state stabilization allows us to attribute the stabilizing effects of chelation exclusively to the transition structure. The importance of chelating ligands in LDA-mediated dehydrobrominations, but not in previously studied reactions of LDA, sheds light on lithium ion chelation.

The consequences of aggregation in organolithium chemistry have been the focus of considerable discussion for over three decades.[1] While most organolithium reactants are aggregated under the conditions employed by synthetic chemists, it is not known in many cases whether the observable aggregates react directly or by first deaggregating to transient lower aggregates or monomers. Moreover, the critical role of solvation is very poorly understood.[2] Reaction rates typically display marked dependencies on the choice of solvent or additive; we offer the relative rate constants shown in parentheses in Chart 1 as representative. To understand organolithium reactivity at even a rudimentary level, one must determine the dependence of the solvation numbers, aggregation states, and relative stabilities of the reactants and the rate limiting transition structure(s) on the solvent structure. In a disturbing number of instances, the discussion focuses upon the effects that each solvent and additive has on the rate limiting transition structures, paying no attention to the ground state. This implicit normalization of all ground states to a single energy—a misconception we have facetiously come to call the "universal ground state"—is completely unjustifiable under normal circumstances. Even the notion that solvent effects are *predominantly* ascribable to differential transition structure solvation would be difficult to justify.[3,4]

We initiated rate and mechanistic studies of the dehydrobromination of (±)-2-*exo*-bromonorbornane (**1**, eq 1) mediated by

$$[(i\text{-Pr})_2\text{NLi·S}]_2 \ (2\text{-}7) \quad (1)$$
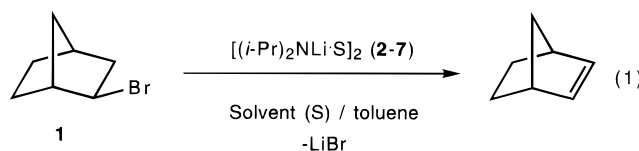
lithium diisopropylamide (LDA) solvated by different monodentate ethereal ligands (disolvated dimers **2**−**7**).[5−7] The dehydrobromination of **1** proceeds without complicating side reactions, allowing the study of the solvent-dependent relative rate constants in terms of reactant and transition structure solvation numbers, aggregation numbers, and relative stabili-

⊗ Abstract published in *Advance ACS Abstracts,* May 15, 1997.

(1) Szwarc, M. *Carbanions, Living Polymers, and Electron Transfer Processes*; Interscience: New York, 1968. *Ions and Ion Pairs in Organic Reactions*; Szwarc, M., Ed.; Wiley-Interscience: New York, 1972; Vols. 1 and 2. *Anionic Polymerization: Kinetics, Mechanism, and Synthesis*; McGrath, J. E., Ed.; American Chemical Society: Washington, 1981, Chapters 1, 2, and 29. Seebach, D. *Angew. Chem., Int. Ed. Engl.* **1988**, *27*, 1624. Seebach, D. In *Proceedings of the Robert A. Welch Foundation Conferences on Chemistry and Biochemistry*; Wiley: New York, 1984. Williard, P. G. In *Comprehensive Organic Synthesis*; Pergamon: New York, 1991; Vol. 1, p 1.

(2) For leading references to rate studies affording insights into transition structure solvation numbers see: (a) Bernstein, M. P.; Collum, D. B. *J. Am. Chem. Soc.* **1993**, *115*, 8008. (b) Schmitz, R. F.; Dekanter, F. J. J.; Schakel, M.; Klumpp, G. W. *Tetrahedron* **1994**, *50*, 5933.

(3) A particularly clear discussion of the relationship between ground state and transition state solvation in organolithium chemistry has been presented: Klumpp, G. W. *Recl. Trav. Chim. Pays-Bas* **1986**, *105*, 1. See also ref 4.

(4) Collum, D. B. *Acc. Chem. Res.* **1993**, *26*, 227.

(5) Lithium dialkylamides are important reagents in synthetic organic chemistry: d'Angelo, J. *Tetrahedron* **1976**, *32*, 2979. Heathcock, C. H. In *Comprehensive Carbanion Chemistry*; Buncel, E., Durst, T., Eds.; Elsevier: New York, 1980; Vol. B, Chapter 4. Cox, P. J.; Simpkins, N. S. *Tetrahedron: Asymmetry* **1991**, *2*, 1. *Asymmetric Synthesis*; Morrison, J. D., Ed.; Academic Press: New York, 1983; Vol. 3, Chapter 1. Snieckus, V. *Chem. Rev.* **1990**, *90*, 879. Juaristi, E.; Beck, A. K.; Hansen, J.; Matt, T.; Mukhopadhyay, M.; Simson, M.; Seebach, D. *Synthesis* **1993**, 1271. Caubère, P. *Chem. Rev.* **1993**, *93*, 2317. Majewski, M.; Gleave, D. M. *J. Orgnomet. Chem.* **1994**, *470*, 1.

(6) Gregory, K.; Schleyer, P. v. R.; Snaith, R. *Adv. Inorg. Chem.* **1991**, *37*, 47. Mulvey, R. E. *Chem. Soc. Rev.* **1991**, *20*, 167.

(7) For selected examples of applications and mechanistic investigations of lithium amide mediated 1,2-eliminations, see: (a) Mass, R. J.; Rickborn, B. *J. Org. Chem.* **1986**, *51*, 1992. (b) Kopka, I. E.; Nowak, M. A.; Rathke, M. W. *Synth. Commun.* **1986**, *16*, 27. (c) Evans, K. L.; Prince, P.; Huang, E. T.; Boss, K. R.; Gandour, R. D. *Tetrahedron Lett.* **1990**, *31*, 6753. (d) Matsuda, H.; Hamatani, T.; Matsubara, S.; Schlosser, M. *Tetrahedron* **1988**, *44*, 2865. (e) Reisdorf, D.; Normant, H. *Organomet. Chem. Synth.* **1972**, *1*, 375.

Chart 1

A (1)   B (1.4)   C (6)   D (36)   E (50)

F (15)   G (1,080)   H (135)   I (8)

J (190)   K (450)   L (600)   M (12)
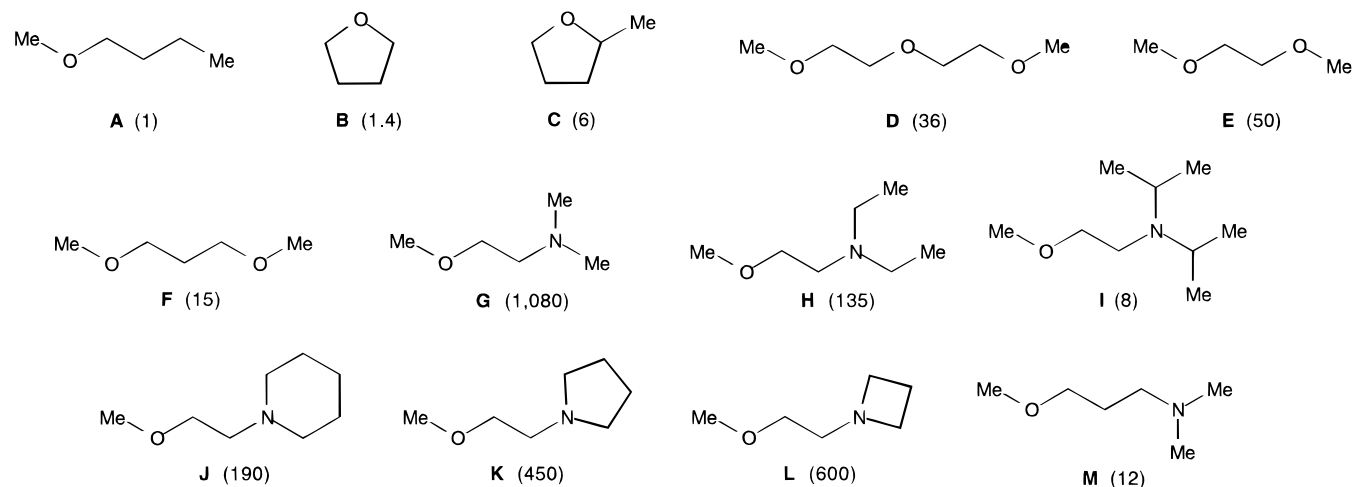
ties.[8,9] The results expose a pivotal role for transition structures bearing monomeric LDA fragments, provide insights into the "chelate effect",[10] and reveal details of transition structure solvation separated from reactant solvation.[3,4]

2; S = *n*-BuOMe
3; S = THF

4; X = OMe
5; X = NMe₂
6; X = NEt₂
7; X = N
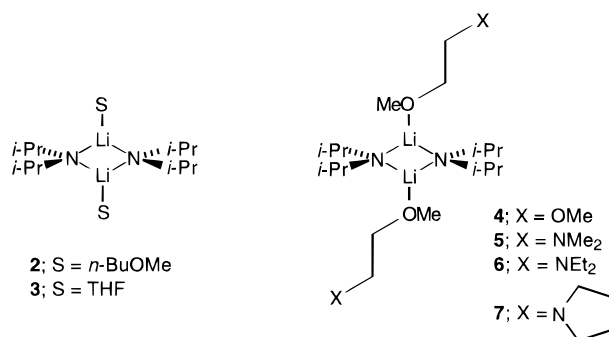
Results

The structures of the LDA dimers **2**−**7** were determined by [6]Li and ^{15}N NMR spectroscopic analyses of [[6]Li,^{15}N]LDA as described in the preceding paper.[11,12] Relative ligand binding constants determined by independent methods in the previous manuscript and as described below are in full accord with the assignment of **4**−**7** as η^1, oxygen-bound solvates.

The rate of LDA-mediated dehydrobrominations of (±)-2-*exo*-bromonorbornane[13] (**1**, eq 1) was monitored via GC analysis of quenched aliquots following the decrease of **1** relative to an internal undecane standard. The LDA was prepared and recrystallized as described previously.[14] The LDA concentrations ([LDA] = 0.025−0.40 M) were maintained high relative to **1** (0.004 M) to ensure pseudo-first-order conditions. These conditions also precluded formation of substantial concentrations of mixed aggregates arising from incorporation of the LiBr

byproduct.[15,16] The ethereal ligand concentrations ([ligand] = 1.0 M−neat) were adjusted with use of toluene as an inert co-solvent.[17] The decay of **1** displayed first-order behavior over >3 half-lives for all LDA−solvent combinations. Substantial kinetic isotope effects ($k_{obsd(H)}/k_{obsd(D)}$ = 1.8−4.0) determined by comparing **1** with the 3,3-dideuterio analog (**1-d₂**)[13] confirmed a rate limiting proton abstraction in all instances. Table 1 compiles reaction orders, activation parameters, isotope effects, and relative solvent binding constants (K_A; *vide infra*) for a variety of LDA/solvent combinations.

Rate Equation: LDA/*n*-BuOMe (2). The pseudo-first-order rate constants for the dehydrobrominations of **1** by LDA in *n*-BuOMe−toluene are independent of [*n*-BuOMe] (Figure 1) and display an approximate half-order dependence on [LDA] (Figure 2, Table 1). The data are consistent with the idealized rate law shown in eq 2. While the LDA order deviates below

$$-d[\mathbf{1}]/dt = k_{obsd}[\mathbf{1}] \qquad (2)$$

such that $k_{obsd} = k'[LDA]^{1/2}[S]^0$

the theoretical value of 0.5, such deviations have been noted in previous rate studies[2a,18] and seem mechanistically inconsequential. The isotope effect (Table 1) is independent of the *n*-BuOMe concentration. Overall, the data are consistent with

(8) Bartsch, R. A.; Lee, J. G. *J. Org. Chem.* **1991**, *56*, 212.

(9) For reviews describing base-mediated eliminations, see: Bartsch, R. A.; Zavada, J. *Chem. Rev.* **1980**, *80*, 453. Caubère, P. *Chem. Rev.* **1993**, *93*, 2317.

(10) Cotton, F. A.; Wilkinson, G. *Advanced Inorganic Chemistry*, 4th ed.; Wiley: New York, 1980; p 71.

(11) Remenar, J. F.; Lucht, B. L.; Collum, D. B. *J. Am. Chem. Soc.* **1997**, *119*, 5567.

(12) Collum, D. B. *Acc. Chem. Res.* **1993**, *26*, 227.

(13) Brown, H. C.; Krishnamurthy, S. *J. Am. Chem. Soc.* **1972**, *94*, 7159. Creary, X.; Hatoum, H. N.; Barton, A.; Aldridge, T. E. *J. Org. Chem.* **1992**, *57*, 1887. See ref 8.

(14) Kim, Y.-J.; Bernstein, M. P.; Galiano-Roth, A. S.; Romesberg, F. E.; Williard, P. G.; Fuller, D. J.; Harrison, A. T.; Collum, D. B. *J. Org. Chem.* **1991**, *56*, 4435.

(15) (a) For an example of autocatalysis of an *N*-alkylation by LiBr, see: Depue, J. S.; Collum, D. B. *J. Am. Chem. Soc.* **1988**, *110*, 5524. (b) For leading references to apparent lithium amide mixed aggregation effects, see: Hall, P.; Gilchrist, J. H.; Collum, D. B. *J. Am. Chem. Soc.* **1991**, *113*, 9571. Romesberg, F. E.; Collum, D. B. *J. Am. Chem. Soc.* **1994**, *116*, 9198. (c) For additional lithium amide mixed aggregation effects, see: Seebach, D. *Synthesis* **1993**, 1271. Cox, P. J.; Simpkins, N. S. *Tetrahedron: Asymmetry* **1991**, *2*, 1. Hilmersson, G.; Davidsson, O. *Organometallics* **1995**, *14*, 912. Ruck, K. *Angew. Chem., Int. Ed. Engl.* **1995**, *34*, 433. Nichols, M. A.; Waldmuller, D.; Williard, P. G. *J. Am. Chem. Soc.* **1994**, *116*, 1153. Goralski, P.; Legoff, D.; Chabanel, M. *J. Organomet. Chem.* **1993**, *456*, 1. Bunn, B. J.; Simpkins, N. S.; Spavold, Z.; Crimmin, M. J. *J. Chem. Soc., Perkin Trans. 1* **1993**, 3113. Strzalko, T.; Seyden-Penne, J.; Wartski, L.; Froment, F.; Corset, J. *Tetrahedron Lett.* **1994**, *35*, 3935. Sorger, K.; Schleyer, P. v. R.; Fleischer, R.; Stalke, E. *J. Am. Chem. Soc.* **1996**, *118*, 6924. Bunn, B. J.; Simpkins, N. S. *J. Org. Chem.* **1993**, *58*, 533. Mair, F. S.; Clegg, W.; Oneil, P. A. *J. Am. Chem. Soc.* **1993**, *115*, 3388. Williard, P. G.; Liu, Q.-Y. *J. Am. Chem. Soc.* **1993**, *115*, 3380. Sugasawa, K.; Shindo, M.; Noguchi, H.; Koga, K. *Tetrahedron Lett.* **1996**, *37*, 7377.

(16) Elimination of 0.1 M **1** by 0.1 M LDA (1.0 equiv) in THF shows no sign of autocatalysis despite the buildup of substantial concentrations of LiBr.

(17) Toluene appears to participate in both the primary and higher solvation shells of lithium ions.[23,41]

(18) Galiano-Roth, A. S.; Collum, D. B. *J. Am. Chem. Soc.* **1989**, *111*, 6772.

Table 1. Summary of Rate Studies for the LDA-mediAted Dehydrobromination of (±)-2-*exo*-Bromonorbornane (eq 1)[a]

entry	ligand (Chart 1)	LDA order	solvent order[b]	$\Delta G°_{act}{}^{a}$ (kcal/mol)	$\Delta H°_{act}$ (kcal/mol)	$\Delta S°_{act}$ (cal/mol·deg)	$K_A(S_\beta/S_\alpha)^{c}$	k_H/k_D
1	**A** (*n*-BuOMe)	0.40 ± 0.04	0	21.1 ± 2.0	13.0 ± 1.1	−31 ± 4	1.00	1.9 ± 0.1
2	**B** (THF)	0.39 ± 0.02	0,1[d]	20.3 ± 0.5	11.5 ± 0.3	−35 ± 1	2.5 ± 0.1	
3	**B** (THF/toluene)	0.48 ± 0.01[e]	0, 1[d]	21.1 ± 1.5[f]	13.1 ± 0.8[f]	−32 ±3[f]	2.0 ± 0.1[e]	
4	**E** (DME)	0.55 ± 0.02	0	19.1 ± 0.1	g	g	0.93±0.14[h]	2.8 ± 0.3
5	**G**	0.55 ± 0.02	0	17.6 ± 0.3	9.1 ± 0.2	−33 ± 1	1.02±0.09	4.3 ± 0.5
6	**K**	0.59 ± 0.02	0	18.0 ± 0.6	9.5 ± 0.3	−34 ± 1	0.81 ± 0.11	4.0 ± 0.5
7	**H**	0.54 ± 0.01	0	18.6 ± 0.3	8.9 ± 0.3	−39 ± 1	0.95 ± 0.15	3.2 ± 0.5

[a] All measurements were made in neat donor solvent at −20 °C unless noted otherwise. [b] Zeroth order is assigned due to the <10% rise in rate over >10-fold changes in donor solvent concentrations. [c] The equilibrium constants ($K_A(S_\beta/S_\alpha)$) for the ligand (S_β) were determined relative to *n*-BuOMe (S_α) at −20 °C according to Scheme 1 and eq 10. [d] See Figure 3. [e] Values measured in 2.0 M THF/toluene solution. [f] Derived by extrapolation to zero free THF concentration (see text). The value of $\Delta G°_{act}$ is obtained from $\Delta H°_{act}$ and $\Delta S°_{act}$. [g] Decomposition at high temperatures and low reactivity at low temperatures precluded determination. [h] Fit to eq 9.
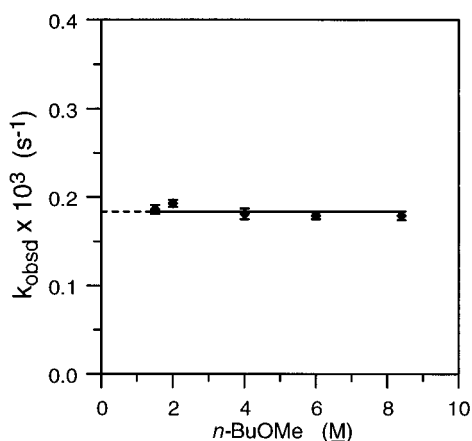

Figure 1. Plot of k_{obsd} versus [*n*-BuOMe] in toluene co-solvent for the elimination of **1** (0.004 M) by LDA (0.10 M) at 20 ± 0.1 °C. The curve depicts the result of an unweighted linear least-squares fit to f(*x*) = *a*.
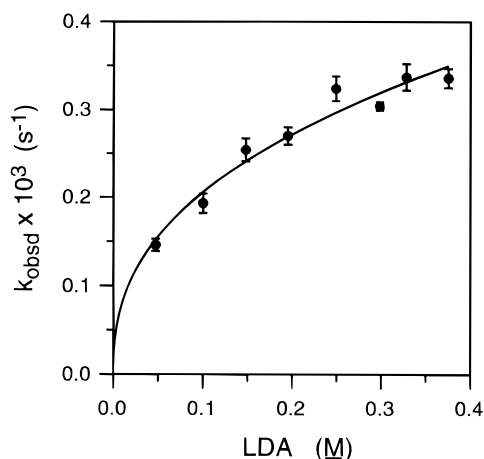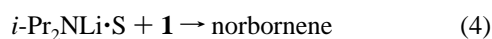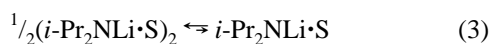

Figure 2. Plot of k_{obsd} versus [LDA] for the elimination of **1** (0.004 M) by LDA in *n*-BuOMe (2.0 M) with toluene co-solvent at 20 ± 0.1 °C. The curve depicts the result of an unweighted nonlinear least-squares fit to f(*x*) = *ax^b* (*b* = 0.40 ± 0.04; see Table 1).

a single reaction pathway involving monosolvated monomers (eqs 3 and 4) at all *n*-BuOMe concentrations.

$$^{1}/_{2}(i\text{-}Pr_2NLi\cdot S)_2 \rightleftharpoons i\text{-}Pr_2NLi\cdot S \qquad (3)$$

$$i\text{-}Pr_2NLi\cdot S + \mathbf{1} \rightarrow \text{norbornene} \qquad (4)$$

Rate Equation: LDA/THF (3). A potentially different mechanistic picture emerges from rate studies in THF solutions. A plot of k_{obsd} vs [THF] in toluene (Figure 3) shows a linear dependence with a significant non-zero intercept. We considered two explanations for this behavior: (1) competing parallel pathways that manifest zeroth- and first-order THF dependen-
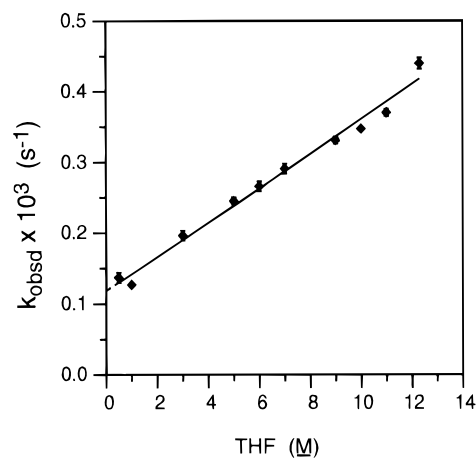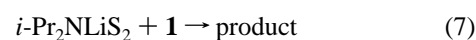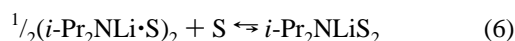

Figure 3. Plot of k_{obsd} versus [THF] in toluene co-solvent for the elimination of **1** (0.004 M) by LDA (0.10 M) at 20 ± 0.1 °C. The curve depicts the result of an unweighted linear least-squares fit to f(*x*) = *a* + *bx*. (See eq 5.) The values of the parameters were calculated to be *a* = 0.24 ± 0.01 and *b* = 1.17 ± 0.08.

cies,[19] or (2) a single pathway that does not formally require a second coordinated THF to lithium at the transition structure, but is sensitive to the surrounding medium. Replacing the toluene co-solvent with either 2,2-dimethyltetrahydrofuran (2,2-Me$_2$THF) or hexane revealed no measurable co-solvent dependence,[20] arguing against long-range medium effects as the source of the [THF] dependence.[21] The fractional LDA orders in 2.0 M THF and 12.3 M (neat) THF implicate dimer−monomer preequilibria at all THF concentrations. The kinetic isotope effects (six measurements in total) increase monotonically over the THF concentration interval from 2.0 M to neat THF (Table 1). The rate data are consistent with the idealized rate law in eq 5 and implicate competing mechanisms based upon monosolvated monomers (eqs 3 and 4) and disolvated monomers (eqs 6 and 7).

$$-d[\mathbf{1}]/dt = k_{obsd}[\mathbf{1}] \qquad (5)$$

such that $k_{obsd} = k'[\text{LDA}]^{1/2} + k''[\text{THF}][\text{LDA}]^{1/2}$

$$^{1}/_{2}(i\text{-}Pr_2NLi\cdot S)_2 + S \rightleftharpoons i\text{-}Pr_2NLiS_2 \qquad (6)$$

$$i\text{-}Pr_2NLiS_2 + \mathbf{1} \rightarrow \text{product} \qquad (7)$$

Rate Equation: LDA/DME (4). The dehydrobromination of **1** is 50-times faster by LDA dimer **4** bearing non-chelated (η^1) DME ligands than by LDA/*n*-BuOMe. Following the loss of **1** at −20 °C, we obtained a zeroth-order DME dependence

(19) A fit of k_{obsd} vs [THF] to the expression $k_{obsd} = k' + k''[\text{THF}]^n$ affords *n* = 1.02 ± 0.15.
(20) At low (<4.0 M) THF concentrations, deviations ascribable to a ligand substitution by 2,2-Me$_2$THF begin to appear.

Scheme 1
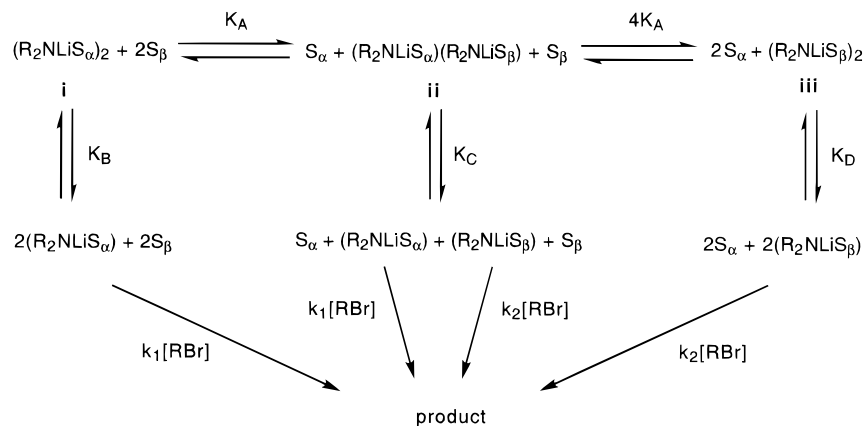
and a fractional LDA order consistent with the idealized rate law in eq 2 and the mechanism generally described by eqs 3 and 4. The substantially higher rate compared with that observed with monodentate ethers strongly implicates the "*i*-Pr$_2$NLi·S" monomer (eq 4) to be **8** bearing a chelating DME. Relative binding constant determinations for *n*-BuOMe and DME (*vide infra*) confirm that the rate accelerations stem entirely from differential transition state energies.
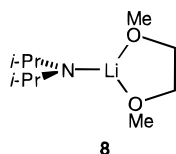
8

Rate Equation: LDA/Amino Ethers (5−7). Systematic variations of the dialkylamine moiety of the amino ethers of general structure R$_2$N(CH$_2$)$_2$OMe revealed highly structure-dependent elimination rates (Chart 1) discussed below.[22] Rate laws for several representative amino ethers confirmed that the mechanism described by eqs 2−4 predominates (Table 1).

Relative Ligand Binding Constants. The NMR spectroscopic studies together with results from previous investigations[2a,23] support the assignment of the disolvated dimers **3−7** bearing η^1 (methoxy-coordinated) rather than chelated ligands. The interpretation of the relative rates hinges upon the assumption that the dimers **3−7** are related by thermoneutral ligand substitution. This was confirmed as described below.[24]

Consider, for example, the equilibria in Scheme 1 and the simple thermochemical picture in Figure 4. (To simplify visual retrieval, the mixed solvate **ii** found in Scheme 1 has been omitted from Figure 4.[25a]) In the limit of either neat S$_\alpha$ or neat S$_\beta$, the two limiting observable species are dimers **i** and **iii**,

(21) During the course of hydrazone metalation rate studies, a seemingly similar first-order dependence on the THF concentration was attributed to medium effects rather than primary shell solvation due to a co-solvent dependence.[18]

(22) Endo, K.; Otsu, T. *Macromol. Rapid Commun.* **1994**, *15*, 233. Poshyachinda, S.; Edwards, H. G. M.; Johnson, A. F. *Polymer* **1991**, *32*, 338. Bywater, S.; Black, P.; Worsfold, D. J.; Schue, F. *Macromolecules* **1985**, *18*, 335. Fraenkel, G.; Geckle, M. J.; Kaylo, A.; Estes, D. W. *J. Organomet. Chem.* **1980**, *197*, 249. Sugahara, K.; Fujita, T.; Watanabe, S.; Hashimoto, H. *J. Chem. Technol. Biotechnol.* **1987**, *37*, 95. Fujita, T.; Watanabe, S.; Suga, K.; Sugahara, K.; Tsuchimoto, K. *Chem. Ind.* **1983**, 167.

(23) Lucht, B. L.; Collum, D. *J. Am. Chem. Soc.* **1996**, *118*, 10707.

(24) A similar binding constant analysis was described previously.[2a] However, several simplifying algebraic assumptions, while not seriously flawed, seem less appropriate in hindsight.

(25) (a) If solvation is non-cooperative, then the ground and transition state corresponding to the mixed solvated LDA will correspond to the mean value of the homosolvated ground states and transition states (respectively) in Figure 4. (b) Benson, S. W. *J. Am. Chem. Soc.* **1958**, *80*, 5151.
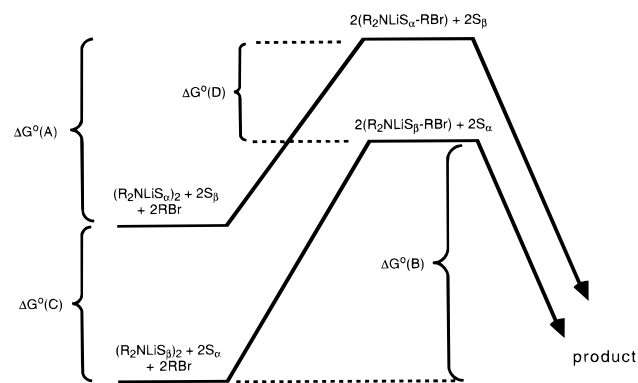
Figure 4.

respectively. The rate constants measured in the neat solvents provide the free energies of activation ($\Delta G°(A)$ and $\Delta G°(B)$). Equation 8 describes k_{obsd} in terms of mechanistic constants and

$$k_{obsd} = \left\{ k_1 K_B^{1/2} + k_2 K_D^{1/2} \left(2K_A \frac{[S_\beta]}{[S_\alpha]} \right) \right\} \times$$
$$\left\{ \frac{A_T}{1 + K_A \frac{[S_\beta]}{[S_\alpha]} + \left(2K_A \frac{[S_\beta]}{[S_\alpha]} \right)^2} \right\}^{1/2} \quad (8)$$

solvent concentrations. (See Supporting Information.) Substituting for $[S_\beta]$ and $[S_\alpha]$ in terms of their mole fractions, X_2 and 1 - X_2, respectively, affords eq 9. Equation 9 includes provisions for the mixed solvate **ii** and allows the binding constant K_A to be found by simple numerical methods.[26] In the event that the rate in neat S$_\alpha$ is not appreciable, eq 9 simplifies to give eq 10.

$$k_{obsd} = \left\{ k_1 K_B^{1/2} + k_2 K_D^{1/2} \left(2K_A \frac{[X_2]}{[1 - X_2]} \right) \right\} \times$$
$$\left\{ \frac{A_T}{1 + K_A \frac{[X_2]}{[1 - X_2]} + \left(2K_A \frac{[X_2]}{[1 - X_2]} \right)^2} \right\}^{1/2} \quad (9)$$

$$k_{obsd} = k_2 K_D^{1/2} \left(2K_A \frac{[X_2]}{[1 - X_2]} \right) \times$$
$$\left\{ \frac{A_T}{1 + K_A \frac{[X_2]}{[1 - X_2]} + \left(2K_A \frac{[X_2]}{[1 - X_2]} \right)^2} \right\}^{1/2} \quad (10)$$

(26) Application of eq 10 causes division by zero at $X_2 = 1$. This problem is adequately alleviated by substituting [1.01 − X_2] for [1 − X_2].
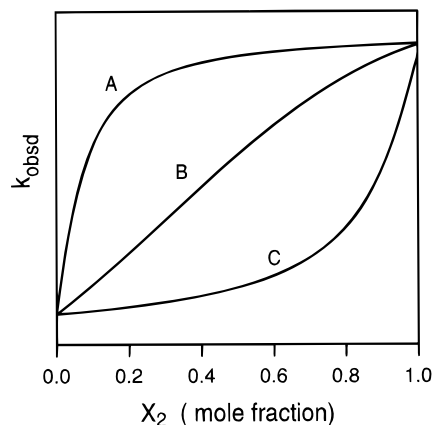
Chelation-Based Stabilization of Transition Structure

J. Am. Chem. Soc., Vol. 119, No. 24, 1997 5577

Figure 5. Predicted rate constants (k_{obsd}) vs mole fraction (X_2) of solvent S_β in co-solvent S_α according to eq 9. Assumptions: (k_{obsd} in neat S_β)/(k_{obsd} in neat S_α) = 10; K_A = 10 (curve A), 1.0 (curve B), and 0.1 (curve C).

The calculated value of K_A provides a measure of the relative free energies of the two ground states corresponding to dimers **i** and **iii** ($\Delta G°$(C), Figure 4). The estimated free energies of activation and relative ground state free energies, in turn, provide the difference in the transition state energies (i.e., $\Delta G°$(D)) to complete the thermochemical picture in Figure 4.

This strategy for investigating LDA solvation offers both qualitative and quantitative insight. Figure 5 shows theoretical curves assuming a 10-fold relative rate difference in neat donor solvents (k_{obsd}(S_β)/k_{obsd}(S_α) = 10) for three relative binding affinities: K_A = 10 (curve A), 1.0 (curve B), and 0.1 (curve C). Curve A will result if the superior donor solvent (S_β) affords kinetically reactive species (as commonly suggested).[25] On the other hand, curve C will result if the stronger solvent (S_α in this case) affords kinetically less reactive species. When the two ligands bind equally, the inflection point will be nearly centered on the x-axis as in curve B.

Before considering the experimental results, it is important to understand the underlying assumptions and approximations. (1) If the magnitudes of the y-intercepts in Figure 5 are fortuitously equivalent, the consequent failure to observe a change in the rate constant renders the method inoperative. In this instance, one might erroneously infer that systematic increases in [S_β] do not affect the reactant structure or mechanism. (2) If the metalation mechanisms that dominate in the neat donor solvents have non-zero solvent reaction orders, the mathematical description would become more complex than described by eq 9. Fortunately, the eliminations described herein are zeroth order in donor solvent (except THF). (3) The precise shape of the function and the accuracy of the value of K_A depend on the assumed solvation states of **i–iii**. If one or more of the solvation state assignments are incorrect, the mathematical form of eq 9 will be incorrect. For hindered lithium amide dimers, the assignments are based upon compelling evidence.[12,27] (4) The model assumes non-cooperative solvation on mixed solvated dimer **ii**. In other words, the dimer subunit exchanges in eq 11 are presumed to be thermoneutral. Recent investigations of LiHMDS support this assumption.[27] The factor of 4 in the second ligand substitution (e.g., 4K_A) stems from statistical contributions in a multi-site ligand substitution.[25b] (5) When measuring pseudo-first-order rate constants with use of solvent mixtures, both solvents must be in excess ($\geq$10 equiv per Li) to avoid substantial errors in the estimates of *free* (as opposed to total) solvent concentration. The error becomes large when $K_A \gg 10$ or $K_A \ll 0.1$ since the
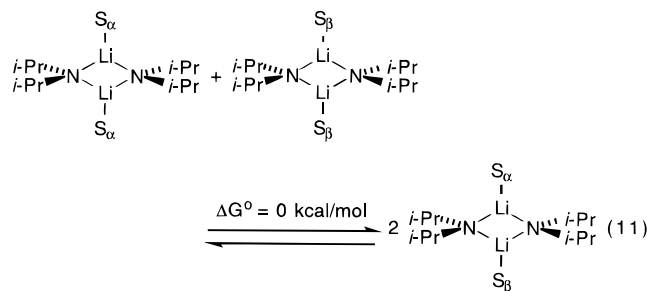
highly curved portion of the function cannot be adequately sampled.

The results are as follows. Figure 6 shows the measured pseudo-first-order rate constants for the elimination of **1** plotted as a function of the Me$_2$NCH$_2$CH$_2$OMe mole fraction in n-BuOMe. Fitting the data to eq 11 (S_α = n-BuOMe and S_β = Me$_2$NCH$_2$CH$_2$OMe) affords K_A(Me$_2$NCH$_2$CH$_2$OMe/n-BuOMe) = 1.02 ± 0.09, corresponding to a ground state free energy difference, $\Delta G°$(C), of <0.05 kcal/mol. Similar investigations of representative amino ethers revealed equivalent binding constants (Table 1).[28] The 25% reduction in the binding constant for pyrrolidine-containing amino ether **K** compared to the other methyl ethers is too small to warrant further discussion.[29]

Temperature-Dependent Rates and Activation Parameters. The solvent-dependent elimination rates were monitored over 30−50 °C temperature ranges to obtain activation enthalpies ($\Delta H°_{act}$) and entropies ($\Delta S°_{act}$) for several cases (Table 1) by using the linear form of the Eyring equation (eq 12). For

$$\ln(k_{obsd}h/kT) = -\Delta H°_{act}/RT + \Delta S°_{act}/R \qquad (12)$$

the reactions described by eqs 3 and 4 involving monosolvated monomer fragments, k_{obsd} is a composite rate constant corresponding to k'[LDA]$^{1/2}$[S]^0 (eq 2). We will exploit the data in the forthcoming discussion to better understand transition structure stabilization by chelation. The data are of reasonable quality as exemplified by Figure 7. We hasten to add that, without a more rigorous treatment,[30] such activation parameters (especially $\Delta S°_{act}$) are susceptible to systematic error and should be viewed with caution.

The activation parameters for the elimination of **1** by LDA in THF and THF−toluene solutions were investigated with three protocols to separate contributions from pathways involving monosolvated monomers (eqs 3 and 4) and disolvated monomers (eqs 6 and 7).

(1) Plotting k_{obsd} vs [THF] (as in Figure 3) with extrapolation to the y-intercepts affords k_{obsd} at *zero* free THF concentration. Plotting the extrapolated values of k_{obsd} vs 1/T at four temperatures afforded the activation parameters corresponding to the zeroth-order pathway (Table 1, entry 3).

(2) Determination of k_{obsd} as a function of temperature in neat THF (Figure 8; Table 1, entry 2) provides values for $\Delta S°_{act}$ and $\Delta H°_{act}$ which, based upon the rate studies described above, represent the total contributions of the pathways involving mono- and disolvated LDA monomers. The substantial decrease in $\Delta H°_{act}$ compared to the value obtained by the protocol

(27) Lucht, B. L.; Collum, D. B. *J. Am. Chem. Soc.* **1995**, *117*, 9863.

(28) The binding constant quoted for DME (K_A, Table 1) has been adjusted to account for the statistical bias imparted by two equivalent methoxy groups.

(29) The measured binding constant can be quite sensitive to the measured end points (rate constants in neat donor solvent). Neglecting the endpoint corresponding to neat MeOCH$_2$CH$_2$N(CH$_2$)$_4$ (in a 9 point plot) affords K_A(MeOCH$_2$CH$_2$N(CH$_2$)$_4$/n-BuOMe) = 1.02 ± 0.10.

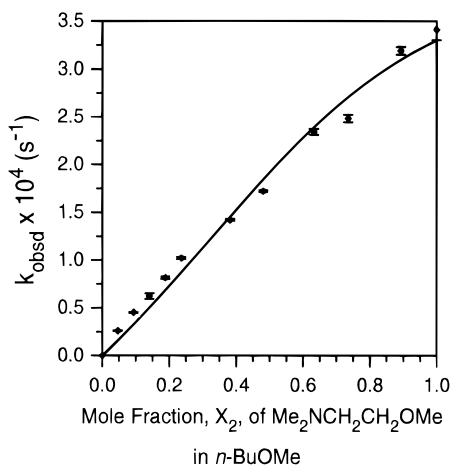(30) Lyons, B. A.; Pfeifer, J.; Peterson, T.; Carpenter, B. K. *J. Am. Chem. Soc.* **1993**, *115*, 2427.

Figure 6. Observed rate constants for dehydrobromination of **1** by LDA vs mole fraction of $Me_2NCH_2CH_2OMe$ (X_2) in *n*-BuOMe under the following conditions: -20 °C; [LDA] = 0.10 M; [**1**] =0.004 M. The curve corresponds to a nonlinear least-squares fit to eq 10, affording $K_A = 1.02 \pm 0.09$ and $k_2K_D = 1.05 \pm 0.02 \times 10^{-2}$.
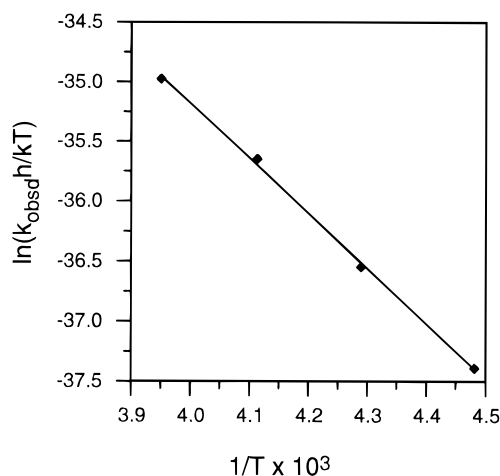

Figure 7. Observed pseudo-first-order rate constants (k_{obsd}) measured as a function of temperature over a 30 °C temperature range (-20 to -50 °C) for the elimination of **1** (0.004 M) by LDA (0.10 M) solvated by $Me_2NCH_2CH_2OMe$ (2.0 M) in toluene. The curve corresponds to a linear least-squares fit to the following equation: $\ln\{k_{obsd}h/kT\} = -\Delta H°_{act}/RT + \Delta S°_{act}/R$. The activation parameters (Table 1) were derived from a non-linear least-squares fit to the following expression: $k_{obsd} = kT/h[\exp(-\Delta H°_{act}/RT)\exp(\Delta S°_{act}/R)]$.

described in (1) is consistent with the emergence of a second, mechanistically distinct pathway.

(3) To dissect the activation parameters into contributions from the parallel reaction pathways, we substitute into the two-term rate equation (eq 5) to obtain eq 13, where $\Delta S°_{act(1)}$ and

$$k_{obsd} = kT/h\{\exp(-\Delta H°_{act(1)}/RT) \exp(\Delta S°_{act(1)}/R)\} + kT/h\{\exp(\Delta H°_{act(2)}/RT) \exp(\Delta S°_{act(2)}/R)\} \quad (13)$$

$\Delta H°_{act(1)}$ correspond to the $k'[LDA]^{1/2}$ term, and $\Delta S°_{act(2)}$ and $\Delta H°_{act(2)}$ correspond to the $k''[THF][LDA]^{1/2}$ term. Since $\Delta S°_{act(1)}$ and $\Delta H°_{act(1)}$ are available by the protocol described in (1), $\Delta S°_{act(2)}$ and $\Delta H°_{act(2)}$ are the remaining unknowns. Plotting k_{obsd} vs T with a nonlinear least-squares fit to eq 13 (Figure 9) affords $\Delta H°_{act(2)} = 11.2 \pm 0.2$ and $\Delta S°_{act(2)} = -36 \pm 1$.

***Syn-Exo* Selectivity.** The *endo-exo* selectivity of the base-mediated $(\pm)$-2-*exo*-bromonorbornane eliminations has been
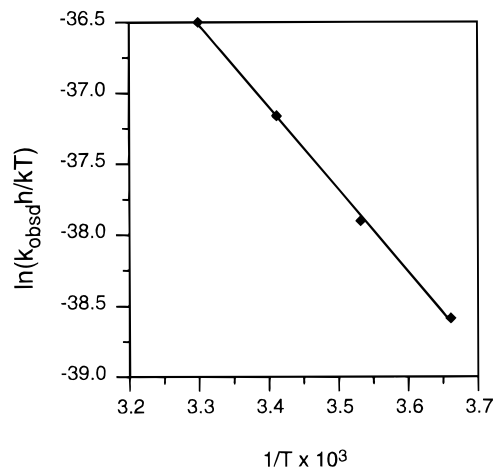

Figure 8. Observed pseudo-first-order rate constants (k_{obsd}) measured as a function of temperature over a 30 °C temperature range (0 to 30 °C) for the elimination of **1** (0.004 M) by LDA (0.10 M) solvated by neat THF. The curve corresponds to a linear least-squares fit to the following equation: $\ln\{k_{obsd}h/kT\} = -\Delta H°_{act}/RT + \Delta S°_{act}/R$. The activation parameters (Table 1) were derived from a nonlinear least-squares fit to the following expression: $k_{obsd} = kT/h[\exp(-\Delta H°_{act}/RT)-\exp(\Delta S°_{act}/R)]$.
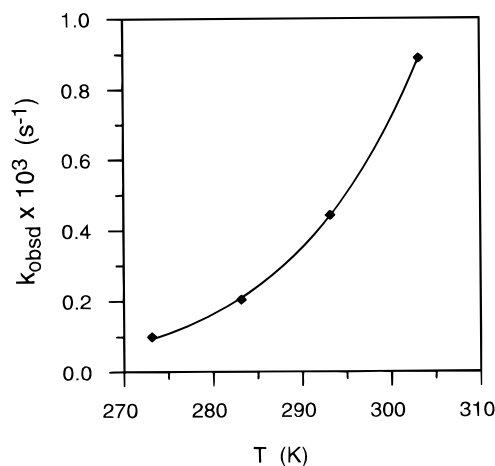

Figure 9. Observed pseudo-first-order rate constants (k_{obsd}) measured as a function of temperature over a 30 °C temperature range (0 to 30 °C) for the elimination of **1** (0.004 M) by LDA (0.10 M) in neat THF. The curve corresponds to a non-linear least-squares fit to the following expression: $k_{obsd} = kT/h\{[\exp(-\Delta H°_{act1}/RT) \exp(\Delta S°_{act1}/R)] + [\exp(-\Delta H°_{act2}/RT) \exp(\Delta S°_{act2}/R)]\}$. The values of the activation parameters $\Delta H°_{act2}$ and $\Delta S°_{act2}$ were determined by fitting the data for the reactions in neat THF to the above equation, where the values of $\Delta H°_{act1}$ and $\Delta S°_{act1}$ are the activation parameters determined from the data extrapolated to free THF concentration.

studied extensively by other investigators.[8,31] Cursory examination of the *exo* selectivity with monodeuterated bromides ***endo-1-d₁*** and ***exo-1-d₁*** reveals >90% *syn-exo* proton abstraction by LDA/*n*-BuOMe, LDA/THF, LDA/DME, and LDA/MeOCH₂-CH₂NMe₂ as shown by GC-MS analysis of the product.[31]

endo*-1-d₁**   ***exo-1-d₁
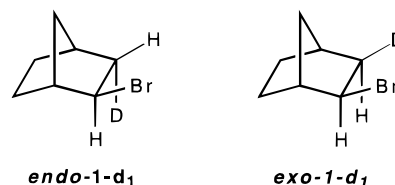
(31) The *endo-exo* selectivities were determined by GC-MS via comparison with authentic samples of norbornene and norbornene-d_1. For related studies see ref 8.

Scheme 2
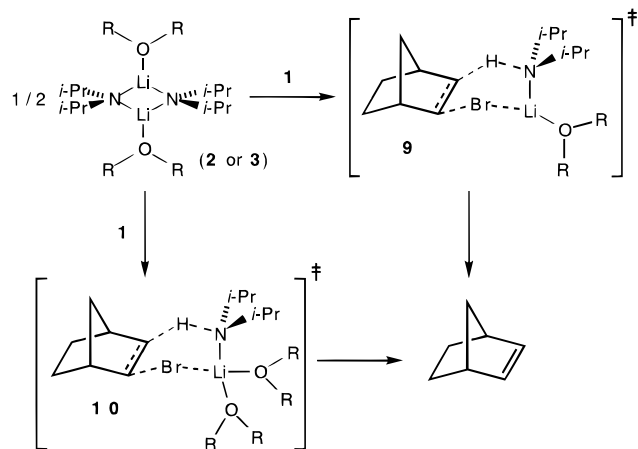
Discussion

In the most general sense, we are interested in understanding the factors that influence lithium amide reactivity. We were drawn to dehydrobrominations by a suggestion of Schlosser and co-workers that LDA-mediated dehydrofluorinations proceed by transition structures based upon LDA open dimers.[7d] Lithium amides and other organolithium open dimers have become a topic of significant attention.[32−34] While an open dimer-based mechanism was not detected in this particular study, the eliminations of (±)-2-*exo*-bromonorbornane (eq 1) provide highly solvent-dependent rates and a mechanistic probe uncomplicated by side reactions. LDA offers substantial advantages over other commonly employed lithium amides and other organolithium reagents in that LDA exists exclusively as a disolvated dimer for a large number of donor solvent structures and concentrations.[11] Our efforts to understand the mechanistic origins of the solvent effects are summarized below.

Mechanism of Dehydrobrominations: The Role of Monodentate Ethereal Ligands. The elimination of **1** by LDA/*n*-BuOMe (**2**) appears to proceed by a single pathway involving a transition structure such as **9** bearing a monosolvated LDA monomer fragment (Scheme 2). The corresponding elimination in THF is more complex. A first-order THF dependence with an appreciable non-zero *y*-intercept (Figure 3), [THF]-dependent isotope effects, and a lack of co-solvent dependence implicate

parallel pathways involving mono- and disolvated transition structures such as **9** and **10**, respectively. The $\Delta H^{\circ}_{\text{act}}$ values for eliminations associated with **9** are indistinguishable for *n*-BuOMe and THF. We infer that any additional stabilization offered by THF compared to *n*-BuOMe[35] in the ground state and transition state cancel. In contrast, $\Delta H^{\circ}_{\text{act}}$ for reaction via **10** where ROR corresponds to THF is ≈2.0 kcal/mol lower than $\Delta H^{\circ}_{\text{act}}$ for reaction via **9**. It seems logical that the superior ligating properties of THF compared to *n*-BuOMe[35] would stabilize such a highly solvated transition structure. The low stabilization when compared with estimated lithium−THF bond enthalpies[27] is consistent with severe steric interactions. The surprising insensitivity of $\Delta S^{\circ}_{\text{act}}$ to the number of ligands in the transition structures is more difficult to explain, but may make sense in the context of open and closed transition structures (*vide infra*).

We do not intend to engage in a discussion of the many classifications of eliminations.[36,37] Nevertheless, some comments about the events occurring at the substrate are warranted. We depict the rate limiting transition structures **9** and **10** as *syn*, *exo*, and cyclic. Several observations confirm the *syn* and *exo* deprotonation, but do not necessarily support cyclic transition structures: (1) Eliminations of ***endo*-1-*d*₁** and ***exo*-1-*d*₁** occur with >90% *syn-exo* proton abstraction. (2) (±)-2-*exo*-iodonorbornane[13] eliminates at nearly the same rate as the bromide **1** ($k_{\text{obsd(I)}}/k_{\text{obsd(Br)}}$ = 2.1 in THF at 20 °C). Orbital alignment and steric factors may be more important than the Li−Br interaction. The low coordination number of putative transition structure **9** seems to demand the existence of a distinct Br--Li interaction, although this may be dogmatic logic. Nevertheless, a change from a cyclic transition structure such as **9** to an open transition structure such as **11** could account for the marginally more negative $\Delta S^{\circ}_{\text{act}}$ associated with a pathway involving an additional ligand. A related issue arises for chelating ligands as described below.
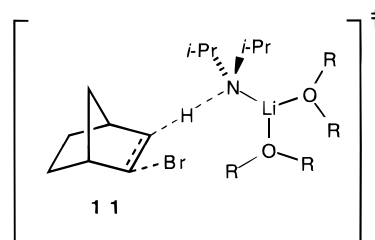
Transition Structure Solvation: Resolving the "Universal Ground State" Problem. The possible importance of transition structures containing disolvated LDA monomer fragments led us to suppose that chelating ligands might offer substantial transition structure stabilization. The typical protocol to test such a hypothesis is to monitor the reaction rates as a function of the chelating ligand. Barring some unlikely coincidences, the reaction rates will vary. However, serious problems arise in the interpretation. The most common practice is to ascribe the rate changes to variable transition structure solvation, paying no attention to solvent-dependent changes in the reactant structures and energies. Inspection of the relative elimination rates in *n*-BuOMe, THF, and 2-MeTHF (in parentheses in Chart

(32) Romesberg, F. E.; Collum, D. B. *J. Am. Chem. Soc.* **1992**, *114*, 2112. Williard, P. G. Unpublished.

(33) Romesberg, F. E.; Collum, D. B. *J. Am. Chem. Soc.* **1994**, *116*, 2166.

(34) Hamatani, T.; Matsubara, S.; Schlosser, M. *Tetrahedron* **1988**, *44*, 2865. Williard, P. G.; Liu, Q.-Y. *J. Am. Chem. Soc.* **1993**, *115*, 3380. Henderson, K. W.; Dorigo, A. E.; Liu, Q-Y.; Williard, P. G.; Schleyer, P. v. R.; Bernstein, P. R. *J. Am. Chem. Soc.* **1996**, *118*, 1339. Bernardi, A.; Capelli, A. M.; Cassinari, A.; Comotti, A.; Gennari, C.; Scolastico, C. *J. Org. Chem.* **1992**, *57*, 7029. Bernardi, F.; Bongini, A.; Cainelli, G.; Robb, M.; Valli, G. S. *J. Org. Chem.* **1993**, *58*, 750. Petasis, N. A.; Teets, K. A. *J. Am. Chem. Soc.* **1992**, *114*, 10328. Gallagher, D. J.; Beak, P. *J. Org. Chem.* **1995**, *60*, 7092. Romesberg, F. E.; Collum, D. B. *J. Am. Chem. Soc.* **1992**, *114*, 2112. Romesberg, F. E.; Collum, D. B. *J. Am. Chem. Soc.* **1994**, *116*, 2166. Romesberg, F. E.; Gilchrist, J. H.; Harrison, A. T.; Fuller, D. J.; Collum, D. B. *J. Am. Chem. Soc.* **1991**, *113*, 5751. Romesberg, F. E.; Collum, D. B. *J. Am. Chem. Soc.* **1994**, *116*, 9187. Bernstein, M. P.; Collum, D. B. *J. Am. Chem. Soc.* **1993**, *115*, 789. Bernstein, M. P.; Collum, D. B. *J. Am. Chem. Soc.* **1993**, *115*, 8008. Bernstein, M. P. Ph.D. Dissertation, Cornell University, Ithaca, NY, 1993. Koch, R.; Wiedel, Anders, E. *J. Org. Chem.* **1996**, *61*, 2523. Pratt, L. M.; Khan, I. M. *Tetrahedron: Asymmetry* **1995**, *6*, 2165. Pratt, L. M.; Hogen-Esch, T. E.; Khan, I. M. *Tetrahedron* **1995**, *51*, 5955. Harder, S.; van Lenthe, J. H.; van Eikema Hommes, N. J. R.; Schleyer, P. v. R. *J. Am. Chem. Soc.* **1994**, *116*, 2508. Ashby, E. C.; Noding, S. A. *J. Org. Chem.* **1979**, *44*, 4371. Shimano, M.; Meyers, A. I. *J. Org. Chem.* **1996**, *61*, 5714. Alvaro, G.; Savoia, D.; Valentini, M. R. *Tetrahedron* **1996**, *38*, 12571. Williard, P. G. Unpublished.

(35) Binding affinities to LiHMDS dimers follow the order THF > MeTHF > *n*-BuOMe.[27]

(36) March, J. *Advanced Organic Chemistry*, 4th ed.; Wiley: New York, 1980; Chapter 17.

(37) For leading references to theoretical investigations of dehydrohalogenations, see: Glad, S. S.; Jensen, F. *J. Org. Chem.* **1997**, *62*, 253. Gronert, S. *J. Org. Chem.* **1994**, *59*, 7046. Dewar, M. J. S.; Yuan, Y.-C. *J. Am. Chem. Soc.* **1990**, *112*, 2088.

Scheme 3
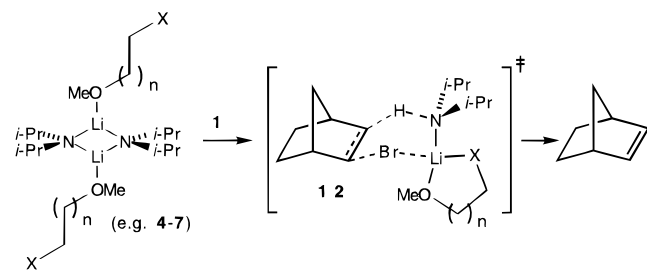
1) suggests the lack of such a simple correlation.[38] By ignoring the solvent effects on the reactants, one implicitly assumes that all ground states are of the same energy. We facetiously call this the "universal ground state". *It is difficult, yet essential, to dissect relative reaction rates into the rate retarding influence of ground state stabilization and the rate accelerating influence of transition state stabilization. Failure to consider both is logically flawed and will lead to invalid conclusions.* More detailed discussions of this problem have been published.[3,4]

We avoided the "universal ground state" assumption in two ways. The simple solution was to choose potentially chelating ligands in which the binding affinities to the LDA dimer can be assumed to be equal. The non-chelated (η^1) DME ligands on LDA dimer **4** should have the same binding constant as *n*-BuOMe. In other words, the substitution of DME for *n*-BuOMe should be thermoneutral. If so, the 50-fold rate acceleration for LDA/DME compared to LDA/*n*-BuOMe can be ascribed to the stabilization of a chelated transition structure such as **12** (Scheme 3). We extended this study to include a variety of methyl ethers bearing potentially chelating pendant groups—so-called "hemilabile ligands" (Chart 1). We have previously shown that even the least hindered trialkylamines are poor ligands for lithium amide dimers.[2a,11,20–23,39–42] This ensures that only the methoxy groups are coordinated in the ground state and that ligand substitution is thermoneutral. Determination of selected rate laws (Table 1) secured the mechanistic homology with LDA/DME (Scheme 3). Thus, we can attribute the marked ligand-dependent rate variations—up to 10^3-fold in optimal cases—to differential transition structure stabilization. It is both interesting and important to note that, had we used potentially chelating diamines, we would have seriously undermined mechanistic interpretations by forfeiting our understanding of relative reactant stabilities.

(38) There are a number of reports where ostensibly weaker solvent–lithium interactions lead to increased overall reaction rates: Apparu, M.; Barrelle, M. *Tetrahedron* **1978**, *34*, 1541. Loupy, A.; Seyden-Penne, J. *Tetrahedron* **1980**, *36*, 1937. Reich, H. J.; Green, D. P.; Phillips, N. H. *J. Am. Chem. Soc.* **1989**, *111*, 3444. Loupy, A.; Seyden-Penne, J.; Tchoubar, B. *Tetrahedron Lett.* **1976**, 1677. Bywater, S.; Worsfold, D. J. *Can. J. Chem.* **1962**, *40*, 1564. Kündig, E. P.; Desobry, V.; Simmons, D. P.; Wenger, E. *J. Am. Chem. Soc.* **1989**, *111*, 1804. Reich, H. J.; Phillips, N. H.; Reich, I. L. *J. Am. Chem. Soc.* **1985**, *107*, 4101. Kim, Y. H.; Choi, J. Y. *Tetrahedron Lett.* **1996**, *37*, 5543. Reich, H. J.; Dykstra, R. R. *Angew. Chem., Int. Ed. Engl.* **1993**, *32*, 1469. See refs 2a, 3, and 18.

(39) For early studies revealing poor coordination of trialkylamines to organolithium aggregates, see: Settle, F. A.; Haggerty, M.; Eastham, J. F. *J. Am. Chem. Soc.* **1964**, *86*, 2076. Lewis, H. L.; Brown, T. L. *J. Am. Chem. Soc.* **1970**, *92*, 4664. Brown, T. L.; Gerteis, R. L.; Rafus, D. A.; Ladd, J. A. *J. Am. Chem. Soc.* **1964**, *86*, 2135. Quirk, R. P.; Kester, D. E. *J. Organomet. Chem.* **1977**, *127*, 111.

(40) For a discussion of steric effects of amines in the context of transition metal ligation see: Seligson, A. L.; Trogler, W. C. *J. Am. Chem. Soc.* **1991**, *113*, 2520. Choi, M.-G.; Brown, T. L. *Inorg. Chem.* **1993**, *32*, 1548. Widenhoefer, R. A.; Buchwald, S. L. *Organometallics* **1996**, *15*, 3534.

(41) Lucht, B. L.; Collum, D. B. *J. Am. Chem. Soc.* **1996**, *118*, 2217.

(42) Bernstein, M. P.; Romesberg, F. E.; Fuller, D. J.; Harrison, A. T.; Collum, D. B.; Liu, Q.-Y.; Williard, P. G. *J. Am. Chem. Soc.* **1992**, *114*, 5100.

Of course, a more direct approach to avoid the "universal ground state" assumption is to determine the relative stabilities of the reactants. We described a method by which the *kinetics* of elimination provide the thermodynamics of solvation. Because of the different inherent reactivities of the dimeric reactants **i–iii** (Scheme 1) coordinated by the solvents S_α and S_β, a plot of k_{obsd} vs solvent mole fraction (X) affords a sigmoidal function (Figure 6). The two *y*-intercepts provide the rate constants for metalations by **i** and **iii** with the corresponding activation energies ΔG°(A) and ΔG°(B) (Figure 4). A nonlinear least-squares fit to eq 9 or eq 10 affords the relative solvent binding constants and the relative stabilities of the ground states based upon reactants **i** and **iii** (ΔG°(C) in Figure 4). Overall, the single plot in Figure 6 provides the relative ground state stabilities *and* transition state stabilities. Results from selected cases confirmed that the hemilabile ligands bearing methyl ether moieties bind equivalently to the LDA dimer. Consequently, this confirms the assumption that the dramatic and variable rate increases observed for DME and a variety of bidentate ligands (Chart 1) stem entirely from differential transition structure solvation.

Transition Structure Solvation: The Chelate Effect. The rate accelerations imparted by DME and related amino ethers (Chart 1) do not derive from a general promotion of high solvation numbers, but from *selective* stabilization of the transition structure *relative to the LDA dimer reactant*. If chelation stabilizes the reactants *and* the transition structures, the sign and magnitude of a DME-induced rate change is not readily predicted. In contrast, the view of differential transition state solvation unobscured by differential ground state solvation effects offers insights into the chelate effect and allows interesting comparisons with quantitative studies of chelate formation on LiHMDS monomers. These are as follows:

(1) Chelate ring size is critical. Hemilabile diethers and amino ethers capable of forming five-membered chelates (**12**, *n* = 1) offer substantial (up to 10^3-fold) rate advantages when compared to *n*-BuOMe. The corresponding six-membered-ring chelates (**12**, *n* = 2) are much less consequential. This is consistent with their low binding affinities to monomeric LiHMDS.[23]

(2) Transition structure stabilization correlates inversely with an increasing bulk of the pendant ligand. For example, the elimination rates for LDA solvated by $MeOCH_2CH_2NR_2$ follow the order $NR_2 = NMe_2 > NEt_2 > N(i\text{-}Pr)_2$. This is consistent with LiHMDS solvation studies. However, we observe some unexpected substituent effects. We predicted that the transition structure stabilization would correlate with the ground state stabilization of chelated lithium amide monomers; the best comparison currently available is with chelated LiHMDS monomers.[23] The relative transition structure stabilizations follow the order $RN(CH_2)_5$ (**J**) < $RN(CH_2)_4$ (**K**) < $RN(CH_2)_3$ (**L**) < $RNMe_2$ (**M**). Binding affinities of related ethylenediamines ($R_2NCH_2CH_2NR_2$) to LiHMDS monomers follow the order $RNMe_2 \approx RN(CH_2)_5 < RN(CH_2)_4 < RN(CH_2)_3$.[23] This dramatic change in the relative ligating strength of the NMe$_2$ moiety may stem from congestion in the transition structure. This can be seen by comparing ligating strength with ligand substitution rates on LiHMDS. While the dipyrrolidinoethane ligand in LiHMDS monomer **13** is more strongly bound than the TMEDA in **14**, the rates of associative ligand substitutions via monomer **15** are much slower than the corresponding substitutions via monomer **16**; the pyrrolidine groups appear to be relatively intolerant of the additional steric congestion occurring upon ligand association. The dehydrobrominations of **1** by LDA are also susceptible to steric congestion associated

with the substrate−amide interactions. These additional steric effects would not be expected to correlate with chelate stability.

13; NR$_2$ = N (pyrrolidinyl)

14; NR$_2$ = NMe$_2$

15; NR$_2$ = N (pyrrolidinyl)

16; NR$_2$ = NMe$_2$
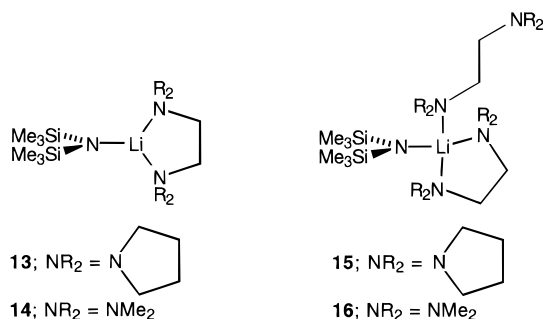
(3) The approximate 20-fold rate enhancement offered by Me$_2$NCH$_2$CH$_2$OMe compared to DME implicates a higher azaphilicity rather than oxaphilicity at the transition structure. While this seems surprising considering the assignment of amino ether solvated LDA as η^1-oxygen-bound dimers (e.g., **5**−**7**), the high azaphilicity is fully compatible with LiHMDS solvation studies. Lithium amide dimers are far too hindered to comfortably support trialkylamine ligands,[2a,11,20−23,39−42] whereas monomers offer a less congested environment.[23] In addition, we found that dialkyl ethers and dialkylamines show indistinguishable affinities for binding to the LiHMDS dimers,[41] while the dialkylamines show a greater tendency than the ethers to bind to the monomers. We concluded that the LiHMDS monomers are more "azaphilic" than the dimers, possibly equating with a stronger Lewis acidity. Interestingly, a similar preference for amine- vs ether-based chelation noted by Reich was accompanied by a *higher* propensity to simultaneously bind an equivalent of HMPA.[43] An enhanced azaphilicity of organolithium monomers and monomer-based transition structures, when compared to higher oligomers, may account for a myriad of di- and polyamine solvation effects on lithium salt structures and reactivities.[4,44]

(4) Although we are skeptical of activation parameters due to their susceptibility to systematic and random error, we attempted to dissect $\Delta G°_{act}$ into $\Delta S°_{act}$ and $\Delta H°_{act}$ to gain a more detailed view of chelation in the transition structure (Table 1). The rate increases observed for LDA solvated by DME and related amino ethers are clearly ascribable to the pendant ligands and reveal factors that affect the chelate stabilities. However, problems arise when we attempt to dissect the chelate effect into separate contributions. For example, the ≈2.0 kcal/mol reduction in $\Delta H°_{act}$ for LDA/DME compared to LDA/*n*-BuOMe stemming from the additional metal−ligand interaction in a chelated transition structure such as **12** is attenuated by the torsional enthalpy loss upon forming the five-membered ring. Similarly, enthalpic gains offered by the second solvent−lithium interaction in di(*n*-BuOMe)-solvated transition structure **10** will be offset by destabilizing solvent−solvent and related steric interactions. It is not obvious that attempting to make such energetic distinctions is a productive exercise. The situation becomes acutely complex when entropy is considered. Comparisons with LDA/*n*-BuOMe reveal that chelation at the transition structure occurs with very little entropic cost despite the anticipated restricted degrees of freedom associated with ring formation. We suspect that open transition structures such as **17** may be intervening, offsetting entropic losses associated with chelate formation. While this model might neatly account for the insensitivity of the $\Delta S°_{act}$ to chelate formation, it also

renders a detailed consideration of $\Delta H°_{act}$ even less appropriate. Lastly, we must confess that all of these inferences are further weakened by the lack of relative ground state enthalpies and entropies; the "universal ground state" emerges again.

1 7
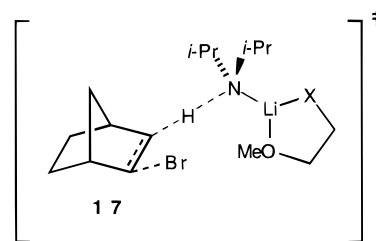
(5) Additional ligating groups only offer rate advantages if the mechanism includes provisions for the additional coordination. The equivalent rates for LDA/diglyme and LDA/DME attest to the lack of η^3 coordination of the diglyme at the transition structure. Diglyme binds as a tridentate ligand on the LiHMDS monomer, but is not unusually stabilizing compared with bidentate diamines.[23] Along a similar vein, LDA-mediated dehydrobrominations and LDA-mediated metalations of *N,N*-dimethylhydrazones both proceed via rate limiting transition structures bearing monosolvated LDA monomer fragments. However, the hydrazones are not metalated via more highly solvated transition structures,[2a,18,42] possibly due to a high steric demand[33] of the hydrazones. Since the potentially polydentate ligands do *not* selectively stabilize the hydrazone metalation transition structures,[13] such ligands offer no rate advantages.[2a,42]

Conclusions

Solvent effects on reaction rates can only be understood with a knowledge of the reaction mechanism(s) as well as the influence of solvation on both the reactant and transition structure stabilities. While this statement seems self-evident, the tendency to ignore solvent-dependent ground state effects−the so called "universal ground state" assumption−is so widespread as to defy explanation. We are unaware of any fundamental principle dictating that transition states are more susceptible to solvation than ground states. For example, the solution phase S$_N$2 reaction is retarded relative to its gas-phase counterpart by disproportionate ground state solvation.[45] The work described herein is not free of simplifying assumptions. However, the protocol employed for separating ground state and transition state solvation to understand the chelate effect has promise, and such distinctions are essential if we are to understand the relationship between solvation, aggregation, and reactivity within organolithium chemistry.

Experimental Section

Reagents and Solvents. *n*-BuOMe, THF, 2-MeTHF, DME, and diglyme were obtained from Aldrich. Vicinal amino ethers **G**, **H**, **I**, **J**, and **K** (see Chart 1) were prepared by *N*-alkylation as described in the previous paper.[46] **F**[47], **L**,[48] and **M**[49] were prepared by (modified) standard procedures. All solvents were distilled by vacuum transfer

(43) Reich, H. J.; Kulicke, K. J. *J. Am. Chem. Soc.* **1996**, *118*, 273. For additional studies of O vs N chelation, see ref 3.

(44) *Polyamine-Chelated Alkali Metal Compounds*; Langer, A. W., Jr., Ed.; American Chemical Society: Washington, DC, 1974.

(45) Craig, S. L.; Brauman, J. I. *J. Am. Chem. Soc.* **1996**, *118*, 6786.

(46) Gibson, M. S. In *The Chemistry of the Amino Group*; Patai, S., Ed.; Wiley: New York, 1968; p 440. Bitsi, G.; Schleiffer, E.; Antoni, F.; Jenner, G. *J. Organomet. Chem.* **1989**, *373*, 343. Spialter, L.; Pappalardo, J. A. *The Acyclic Aliphatic Tertiary Amines*; McMillan; New York, 1965; pp 14−29.

(47) Noyes, A. A. *Am. Chem. J.* **1897**, *19*, 766.

(48) Sammes, P. G.; Smith, S. *J. Chem. Soc., Perkin Trans. 1* **1984**, 2415.

(49) Pine, S. H.; Sanchez, B. L. *J. Org. Chem.* **1971**, *36*, 829 and references cited therein.

(50) McEwen, W. E.; Janes, A. B.; Knapczyk, J. W.; Kyllingstad, V. L.; Siau, W.-I.; Shore, S.; Smith, J. H. *J. Am. Chem. Soc.* **1978**, *100*, 7304.

from sodium benzophenone ketyl. The hydrocarbon stills contained 1% tetraglyme to dissolve the ketyl. (±)-2-*exo*-Bromonorbornane and the deuterated derivatives were prepared according to literature methods.[13] The LDA was prepared as a solid with commercial *n*-BuLi (Aldrich) and purified by the standard literature procedure.[14] The diphenylacetic acid used to check solution titers[51] was recrystallized from methanol and sublimed at 120 °C under full vacuum. Air- and moisture-sensitive materials were manipulated under argon or nitrogen following standard glovebox, vacuum line, and syringe techniques.

Kinetics. For a kinetic run corresponding to a single rate constant, a relatively concentrated (0.5−0.8 M) stock solution of LDA in a ligand−toluene solution was prepared and titrated to determine the precise concentration. The solution was diluted to a concentration appropriate for the particular series and titrated a second time. A series of oven-dried, nitrogen-flushed 5-mL serum vials (5−10 per rate constant) fitted with stir bars were charged with the LDA stock solution and brought to the desired temperature (±0.2 °C) with use of a constant−temperature bath fitted with a National Bureau of Standards thermometer. The (±)-2-*exo*-bromonorbornane was added as a 0.047 M stock solution in the appropriate ligand−toluene mixture containing undecane (0.047 M) as a GC standard. The vessels were periodically quenched with 1:1 H_2O−THF at intervals chosen to ensure an adequate sampling of each of the first three half-lives. The quenched aliquots were extracted into Et_2O, and the extracts were analyzed via capillary

GC. Use of a Hewlett Packard GC fitted with an autoinjector and a 60-m DB-5 column (J & W Scientific) provided excellent reproducibility. The eliminations were monitored by following the decrease of the (±)-2-*exo*-bromonorbornane (**1**) relative to the internal undecane standard. Following the formation of the norbornene afforded equivalent rate constants (±10%). Rate constants were determined by numerical integration with a convergence protocol using the Scientist distributed by MicroMath. Nonlinear least-squares fits using the integral form of the rate laws afforded numerically indistinguishable results. The reported errors correspond to one standard deviation. The observed rate constants were shown to be reproducible within ±5%.

Supporting Information Available: Plots and tables of rate data (19 pages). See any current masthead page for ordering and Internet access instructions.

---

(51) Kofron, W. G.; Baclawski, L. M. *J. Org. Chem.* **1976**, *41*, 1879.

JA970030A